RESEARCH ARTICLE

Reductive enzymatic dynamic kinetic resolution affording 115 g/L (*S*)-2-phenylpropanol

Christian Rapp[1], Simone Pival-Marko[1,3], Erika Tassano[2], Bernd Nidetzky[1,3] and Regina Kratzer[1]*

Abstract

Background: Published biocatalytic routes for accessing enantiopure 2-phenylpropanol using oxidoreductases afforded maximal product titers of only 80 mM. Enzyme deactivation was identified as the major limitation and was attributed to adduct formation of the aldehyde substrate with amino acid residues of the reductase.

Results: A single point mutant of *Candida tenuis* xylose reductase (*Ct*XR D51A) with very high catalytic efficiency ($43 \cdot 10^3$ s^{-1} M^{-1}) for (*S*)-2-phenylpropanal was found. The enzyme showed high enantioselectivity for the (*S*)-enantiomer but was deactivated by 0.5 mM substrate within 2 h. A whole-cell biocatalyst expressing the engineered reductase and a yeast formate dehydrogenase for NADH-recycling provided substantial stabilization of the reductase. The relatively slow in situ racemization of 2-phenylpropanal and the still limited biocatalyst stability required a subtle adjustment of the substrate-to-catalyst ratio. A value of 3.4 g$_{substrate}$/g$_{cell-dry-weight}$ was selected as a suitable compromise between product *ee* and the conversion ratio. A catalyst loading of 40 g$_{cell-dry-weight}$ was used to convert 1 M racemic 2-phenylpropanal into 843 mM (115 g/L) (*S*)-phenylpropanol with 93.1% *ee*.

Conclusion: The current industrial production of profenols mainly relies on hydrolases. The bioreduction route established here represents an alternative method for the production of profenols that is competitive with hydrolase-catalyzed kinetic resolutions.

Keywords: Enantiopure 2-aryl-1-propanol, Reductive dynamic kinetic resolution, Biocatalyst stability, Aldo–keto reductase engineering

Highlights

● The D51A mutant of *Candida tenuis* xylose reductase showed a 270-fold higher enzymatic activity and improved enantioselectivity for (*S*)-2-phenylpropanal.

● Use of a whole-cell catalyst stabilized the enzyme > 1000-fold under reaction conditions.

● Efficient kinetic resolution of racemic 2-phenylpropanal by the whole-cell catalyst was demonstrated.

● (*S*)-2-phenylpropanol was produced with a titer of 843 mM (115 g/L) and 93.1% *ee*.

● The substrate-to-biocatalyst ratio was the main factor determining the enantiopurity and final titer of the product.

Background

2-Aryl-1-propanols are crucial synthons of profen-type non-steroidal anti-inflammatory drugs (NSAIDs) [1]. The simplest representative of this class, 2-phenylpropanol, has an odor resembling lilac or hyacinth, and is used as a fragrance ingredient in personal care products, as well as a precursor in the synthesis of further fragrances [2,

*Correspondence: regina.kratzer@tugraz.at
[1] Institute of Biotechnology and Biochemical Engineering, Graz University of Technology, NAWI Graz, 8010 Graz, Austria
Full list of author information is available at the end of the article

Rapp *et al. BMC Biotechnol*   (2021) 21:58

Page 2 of 13

3]. The different biological activities and odors of *R*- and *S*-profens have inspired studies on the production of optically pure 2-aryl-1-propanols. A number of biocatalytic routes have been proposed over the years, including kinetic resolutions by hydrolases, nitrile-converting enzymes or oxidases, asymmetrization of prochiral precursors through enzymatic decarboxylation, and isomerization by styrene oxide isomerase. Kinetic resolutions using hydrolases and oxidoreductases are the two most mature strategies (reviewed in [4]). The economic attractiveness of kinetic resolutions, which are restricted to maximally 50% yield, can be increased by in situ racemization of the unused antipode, resulting in dynamic kinetic resolutions (DKR). DKR strategies exploiting hydrolases and oxidoreductases make use of the relatively fast racemization of 2-aryl-1-propanoic acids/esters and 2-aryl-1-propanals (Fig. 1). Hydrolase-catalyzed kinetic resolutions were the first biocatalytic routes towards enantiopure profens, and numerous lipases and esterases have been tested for their enantioselectivities towards several profens [5]. Product concentrations of 0.5 M and enantiopurities of up to 99% *ee* were reported, leading to the application of hydrolases at the industrial scale [6, 7]. Although hydrolases remain attractive in terms of their process performance, they offer limited opportunities to valorize intellectual property [4]. Oxidoreductases are an interesting alternative, but the published biocatalytic routes for accessing chiral 2-aryl-1-propanols using oxidoreductases show markedly lower product concentrations of maximally 80 mM [4, 8–17]. Here, we report a reductive enzymatic dynamic kinetic resolution for the preparation of (*S*)-2-phenylpropanol. The xylose reductase from *Candida tenuis* (*Ct*XR, aldo–keto reductase superfamily) showed a basal activity with *rac*-2-phenylpropanal and moderate preference for the (*S*)-enantiomer. We investigated five enzyme variants with single point mutations in close vicinity to the stereocenter of 2-phenylpropanal. The D51A mutant of *Ct*XR showed high catalytic activity with excellent enantioselectivity for (*S*)-2-phenylpropanal, and was integrated into a reductive whole-cell catalyst based on *E. coli*. Reaction optimization resulted in high enantioselectivity and product concentration at full conversion. The reductive enzymatic dynamic kinetic resolution established in this study is comparable with lipase-based processes in terms of product concentration, offering a viable alternative for industrial applications.

Results

*Ct*XR, which converts xylose to xylitol in the central sugar metabolism of *Candida tenuis*, is a member of the aldo–keto reductase (AKR) superfamily. Like many other AKRs, *Ct*XR has broad substrate specificity, and several

substrate-binding site mutants with improved specificity for aromatic ketones were used in the synthesis of (*R*)-ethyl mandelates and (*S*)-phenylethanols [18, 19]. However, the application of *Ct*XR as an industrial biocatalyst was hindered by its moderate catalytic activity and low stability. Motivated by a moderate intrinsic activity of wild-type *Ct*XR on *rac*-2-phenylpropanal ($k_{cat}/K_{m,rac}$ 130 s^{-1} M^{-1}, k_{cat} 0.05 s^{-1}), we tested a number of single point mutations targeting the substrate-binding site for their effects on the activity and enantioselectivity of the enzyme in the reduction of 2-phenylpropanal.
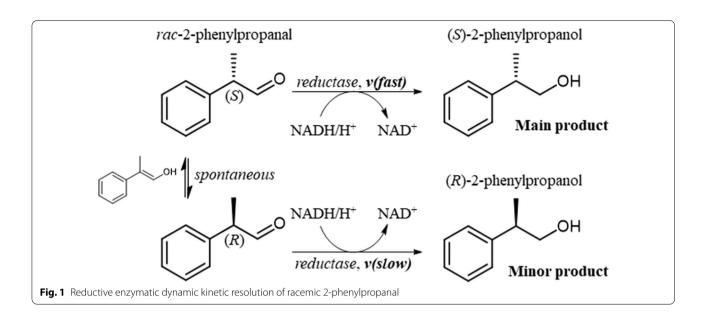
CtXR mutants

The substrate-binding cavity of aldo–keto reductases is mainly formed by residues from three large and flexible loops [20, 21]. Loop flexibility provides the structural basis for the relaxed substrate specificity, but complicates rational engineering [22]. A model of the binding mode of the natural substrate D-xylose (open chain form) indicated that the C-1 of xylose is positioned within hydride-transfer distance above the C-4 of nicotinamide, with a hydrogen bond between the carbonyl oxygen and the general acid catalyst Tyr-52. In this model, the aldehyde hydrogen was oriented towards the indole ring of Trp-24 and the C-2 hydroxyl interacted with Asn-310, while the hydroxyl groups of C3, C4 and C5 interacted with Asp-51 [23]. Here, we probed wild-type *Ct*XR and individual point mutants of the main substrate recognition residues Trp-24, Asn-310 and Asp-51 as catalysts for the reduction of 2-phenylpropanal. The replacement of Trp-24 with smaller phenylalanine and tyrosine was previously shown to increase enzyme activity on bulky ketone substrates [18, 24]. Interaction between the Nδ1 of Asn-310 and the C-2(*R*) hydroxyl of sugars is considered the basis for substrate discrimination in *Ct*XR [23, 24]. Asp-51 accounts for a major part of the relative polarity of the binding site, and its substitution with alanine led to improved activity with the aromatic ketone *o*-chloroacetophenone [19].

Reduction of 2-phenylpropanal by *Ct*XR variants

Table 1 summarizes the steady-state kinetics of NADH-dependent reduction of racemic and (*S*)-2-phenylpropanal by wild-type *Ct*XR and the substrate-binding-site mutants.

Racemic substrate. The wild-type enzyme showed a $K_{m,rac}$ value of 350 μM and a k_{cat} value of 0.05 s^{-1}, corresponding to a specificity constant ($k_{cat}/K_{m,rac}$) of 130 s^{-1} M^{-1}. The mutants W24F and W24Y displayed only 8 to 10% of the wild-type activity. Although the N310A mutant had a specificity constant similar to the wild type, the N310D mutant showed no activity. *Ct*XR D51A stood out with a $K_{m,rac}$ value of 170 μM

Rapp *et al. BMC Biotechnol*   (2021) 21:58

Page 3 of 13

Fig. 1 Reductive enzymatic dynamic kinetic resolution of racemic 2-phenylpropanal

and a k_{cat} value of 4.8 s^{-1}, corresponding to a $k_{cat}/K_{m,rac}$ of 28·10^3 s^{-1} M^{-1}. Hence, replacement of the charged aspartic acid with alanine led to 215-fold higher catalytic efficiency compared to the wild type. Conversely, introduction of an additional aspartic acid in the substrate-binding pocket (N310D) completely abolished enzyme activity with 2-phenylpropanal. Enlargement of the substrate binding pocket by replacement of the bulky Trp-24 decreased the enzyme's activity towards 2-phenylpropanal.

(S)-2-phenylpropanal. Kinetic parameters obtained with the racemic substrate and (*S*)-2-phenylpropanal were used to calculate the optical preference ratio $(k_{cat}/K_{m,S})/(k_{cat}/K_{m,rac})$ (Table 1). The wild type showed a ratio of 1.23 with a preference for the *S*-enantiomer. The D51A mutant showed a ratio of 1.54 and hence a stronger preference for the *S*-enantiomer. The W24F, W24Y and N310A mutants displayed ratios < 1, suggesting a preference for the *R*-enantiomer. It should be noted that the *Ct*XR mutants showed 35 to 100-fold reduced catalytic activity towards the natural substrate xylose [24].

We used isolated *Ct*XR D51A in bioreductions of 0.5 mM *rac*-2-phenylpropanal. The substrate (log*P* 2.11, https://scifinder.cas.org/) displayed a maximal solubility of 0.5 mM in the buffer (50 mM potassium phosphate, pH 7.0 with 25% DMSO). Product concentrations and *ee* values obtained at enzyme concentrations between 360 and 0.6 U/mL are listed in Table 2. The product *ee* values increased with decreasing amounts of the enzyme. Unexpectedly, the reactions stopped after approximately 1 h and maximal product concentrations of only ∼ 80 µM were achieved (for a time course see the Additional file 1: Fig. S1). We suspected that enzyme deactivation caused

the low conversions and decided to use a whole-cell biocatalyst expressing *Ct*XR D51A for further experiments.

Optimization of *rac*-2-phenylpropanal reduction using whole cells of *E. coli* co-expressing *Ct*XR D51A and a yeast formate dehydrogenase

Bioreductions were accomplished using whole cells of transgenic *E. coli* that were lyophilized and rehydrated in phosphate buffer. The phenylpropanal reductase and formate dehydrogenase activities of the whole-cell biocatalyst were 2200 and 154 U/g$_{CDW}$, respectively (the *rac*-2-phenylpropanal reduction activity was determined with 0.5 mM *rac*-2-phenylpropanal). Addition of the biomass to reaction mixtures with a final substrate concentration of more than 100 mM led to emulsification [25]. A substrate concentration of 100 mM was converted by 4 and 10 g$_{CDW}$/L of the whole-cell biocatalyst to 41 and 67 mM (*S*)-phenylpropanol with *ee*-values of 95.3 and 62%, respectively (Fig. 2). Next, we optimized the catalyst loading (20 and 40 g$_{CDW}$/L), substrate concentration (1 and 2 M), NAD$^+$ concentration (3, 6, 8, 10, 12 and 14 mM) and cyclodextrin addition (38 and 75 mM) (Table 3). Our primary goal was a high product concentration, as the substrate had shown a strong deactivating effect on the isolated enzyme. Secondary goals were high product enantiopurity and a high conversion ratio. We increased the substrate concentration to 1 M at 20 and 40 g$_{CDW}$/L catalyst loading. Product enantiopurity and conversion increased with higher biocatalyst concentration. A catalyst loading of 20 g$_{CDW}$/L led to an *ee* value of 95.1%, but the conversion ratio fell to 23%. Increasing the catalyst loading to 40 g$_{CDW}$/L decreased the *ee* value to 92.2% but achieved 51% conversion (Table 3, entries

Rapp *et al. BMC Biotechnol*   (2021) 21:58

Page 4 of 13

with 3 mM NAD$^+$). A substrate concentration of 2 M was too high, resulting in only low conversions of ~30%. The step-wise addition of substrate at 0, 2 and 4 h corresponding to a total substrate concentration of 1 M led to conversions and product *ee*-values comparable to batch conversions (Table 3). We added higher concentrations of the coenzyme NAD$^+$ (6 to 14 mM) to reactions with 40 g$_{CDW}$/L and 1 M substrate to further push the reaction towards full conversion. With 10 and 12 mM NAD$^+$, conversion ratios of up to 84% were reached, with *ee* values of 92–93% (Table 3). The effects of catalyst loading and NAD$^+$ concentration are summarized in the Additional file 1: Fig. S2. The addition of 75 mM 2-hydroxypropyl-β-cyclodextrin was previously shown to boost bioreductions [19]. Here, the addition of 38 or 75 mM 2-hydroxypropyl-β-cyclodextrin had a positive effect on reactions with a catalyst loading of 20 g$_{CDW}$/L, but it had of no significant effect on bioreductions of 1 and 2 M 2-phenylpropanal (Table 3).

Reproducibility, recovery and by-products

Replicate bioreductions (N=7) with 40 g$_{CDW}$/L and 6 mM NAD$^+$ showed high reproducibility with a mean conversion ratio of 62% and a standard deviation of 2.4%. The enantiomeric excess was 93.3±1.1%. The formation of broad peaks prevented the quantification of the aldehyde substrate by chiral reversed-phase HPLC. We therefore additionally analyzed the bioreduction samples by chiral GC-FID (Additional file 1: Fig. S4). The high reactivity of the substrate 2-phenylpropanal prompted us to investigate possible by-products generated through chemical or bio-chemical side-reactions. It was previously shown that acetophenone is formed through the degradation of *rac*-2-phenylpropanal by atmospheric oxygen [26]. Hydrophobic compounds were extracted from two reaction mixtures (1 M *rac*-phenylpropanal,

40 g$_{CDW}$/L catalyst, 6 mM NAD$^+$, 1 mL volume per reaction), after which the solvent, and possibly unreacted 2-phenylpropanal (bp 92 – 94°), were removed under reduced pressure. The concentrate with a weight of 203 mg was composed of 86% 2-phenylpropanol, 7% acetophenone and 7% ethyl acetate (extractant) according to ^{1}H-NMR (Additional file 1: Fig. S5). We found trace amounts of 1-phenylethanol, the enzymatic reduction product of acetophenone [27]. Notably, no 2-phenylpropanal was found. The substrate was in a chemical equilibrium between *rac*-2-phenylpropanal and its corresponding hydrates. The previously reported enzymatic oxidation of 2-phenylpropanal hydrates to the corresponding carboxylic acids was not observed [12, 28], and no enol or aldol isoforms of the substrate were detected. The HPLC, GC and NMR analyses are shown in Additional file 1: Sects. 4, 5 and 6, respectively. The loss of substrate/product with the biomass was approximately 15% under the described reaction conditions (data not shown).

Table 2 Conversions and product *ee*-values for the reduction of *rac*-2-phenylpropanal by isolated *Ct*XR D51A.[a,b]

*Ct*XR (U/mL)[c]	Phenylpropanol (μM)	*ee* (S)-Phenylpropanol (%)
D51A (20)	76 ± 3	41 ± 4
D51A (3.4)	51 ± 5	98 ± 2
D51A (0.6)	13 ± 5	99.1 ± 0.3

[a] NAD$^+$ concentration 0.7 mM, reaction time 2 h. [b]The phenylpropanol concentrations were measured by HPLC, the data represent the mean values of two reaction replicates and standard deviations from the mean. [c]The enzyme activity (U/mL) was measured with 0.5 mM *rac*-2-phenylpropanal

Table 1 Apparent kinetic parameters of wild-type *Ct*XR and substrate-binding-site mutants in the NADH-dependent reduction of racemic and (S)-2-phenylpropanal[a]
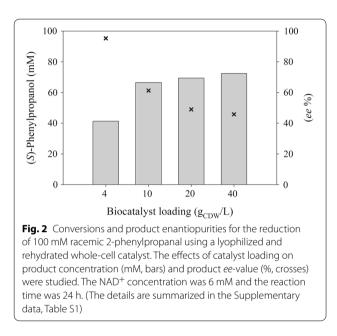
*Ct*XR	*rac*-2-phenylpropanal		(S)-2-phenylpropanal		Optical preference ratio
	$k_{cat}/K_{m,rac}$ (s^{-1} M^{-1})	$K_{m,rac}$ (μM)	$k_{cat}/K_{m,S}$ (s^{-1} M^{-1})	$K_{m,S}$ (μM)	(S)-aldehyde / racemic aldehyde
wild-type	130	350	160	450	1.23
D51A	28·10^3	170	43·10^3	120	1.54
W24F	13[b]	N/A	12	N/A	0.92
W24Y	10[b]	N/A	9	N/A	0.90
N310A	88	280	68	330	0.77
N310D	no activity	no activity	no activity	no activity	-

[a] The kinetic parameters were obtained using non-linear least-squares fitting of the experimental data to the Michaelis–Menten equation in SigmaPlot 2006 (version 10.0 for Windows). [b]When limited substrate solubility prevented saturation of the enzyme, k_{cat}/K_m was calculated from the slope of the Michaelis–Menten plot where the rate is linearly dependent on the substrate concentration. N/A not applicable

Rapp *et al. BMC Biotechnol*   (2021) 21:58

Page 5 of 13

Discussion

Literature survey

A literature survey yielded 13 examples of enantioselective bioreductions of 2-phenylpropanal using free or immobilized enzymes (Table 4). Previous studies investigated bioreduction catalysts (soluble enzymes discussed in entries 1–5, 8–10, 12, 13; immobilized enzymes in entries 6,7,11) in the kinetic resolution of *rac*-2-phenylpropanal (entries 4, 6–11). Most enantioselective enzymes preferred the (*S*)-aldehyde (entries 1–8, 10). Rocha-Martín et al. [13] reported that the ADH from *Thermus thermophilus* HB27 exhibits anti-Prelog specificity (entry 11). Dong et al. [8] used directed evolution on an ADH from *Thermoanaerobacter brockii*, which displayed moderate Prelog-type selectivity, to improve the formation of (*S*)- and (*R*)-alcohols (entries 8, 9). HLADH was used in most studies due to its enantioselectivity, substrate tolerance up to a concentration of 165 mM, and usefulness in coupled substrate strategies (oxidation of cheap alcohols for NADH-recycling). Most other selective ADHs stem from thermophilic organisms and display intrinsically high stability in adverse reaction media. The low number of reported enzymes and the low obtained product titers indicated that the reactive aldehyde substrate generally inactivates the enzymes [29]. Remarkably, the often-used host *E. coli* shows native activity towards 2-phenylpropanal (entry 14) [30], which was traced back to the tetrameric ADH of *E. coli* (entry 12) [1, 31]. Buffered solutions containing water-soluble co-solvents (also used as sacrificial substrates for NADH recycling) were also used in many studies, whereby the aqueous phase enabled the racemization of the substrate. The highest published product concentration of 82 mM was achieved in a 47:63 buffer/isopropyl ether mixture (entry 4) [16].

Fig. 2 Conversions and product enantiopurities for the reduction of 100 mM racemic 2-phenylpropanal using a lyophilized and rehydrated whole-cell catalyst. The effects of catalyst loading on product concentration (mM, bars) and product *ee*-value (%, crosses) were studied. The NAD^+ concentration was 6 mM and the reaction time was 24 h. (The details are summarized in the Supplementary data, Table S1)

Table 3 Conversions and product ee-values for the reduction of rac-2-phenylpropanal using a lyophilized and rehydrated whole-cell biocatalyst. The effects of catalyst loading, substrate concentration, coenzyme concentration and the addition of HBC (2-hydroxypropyl-β-cyclodextrin) were investigated.[a,b]

Catalyst loading (g_{CDW}/L)	*rac*-2-Phenylpropanal (M)	NAD^+ (mM)	HBC (mM)	Phenylpropanol (mM)	*ee* of (*S*)-Phenylpropanol (%)
20	1	3	0	234 ± 16	95.1 ± 0.0
20	1	3	38	401 ± 10	94.1 ± 0.0
20	1	3	75	406 ± 2	93.3 ± 0.1
40	1	3	0	506 ± 14	92.2 ± 0.0
40	1	6	0	619 ± 24[c]	93.3 ± 1.1[c]
40	1 M fed-batch	6	0	611 ± 12	94.0 ± 0.1
40	1	8	0	662 ± 9	94.1 ± 0.1
40	1	10	0	843 ± 31	93.1 ± 0.2
40	1	12	0	839 ± 36	92.9 ± 0.1
40	1	14	0	765 ± 31	92.3 ± 0.1
40	1	6	38	634 ± 8	94.3 ± 0.2
40	1	6	75	598 ± 7	92.9 ± 0.2
40	2	6	0	571 ± 10	95.4 ± 0.1
40	2	6	38	633 ± 2	93.4 ± 0.5
40	2	6	75	637 ± 22	92.2 ± 0.2

[a] Reaction time 48 h. [b]The data represent the mean values and deviations from the mean of two reaction replicates. [c]The data represent the mean values and standard deviations of 7 reaction replicates

Rapp *et al. BMC Biotechnol* (2021) 21:58

Page 6 of 13

Reduction of *rac*-2-phenylpropanal by *Ct*XR variants

We investigated five enzyme variants with single point mutations in close vicinity to the stereocenter of 2-phenylpropanal (Table 1). Replacement of the charged Asp-51 with alanine substantially improved the enzyme's activity. The catalytic efficiency increased 215-fold for *rac*-2-phenylpropanal and 270-fold for the (*S*)-aldehyde compared to the wild type (Table 1). Similarly, the catalytic efficiency in the reduction of *o*-chloroacetophenone was improved 13-times by the D51A mutation [19], which was accompanied by a 50-fold decrease in the conversion of the native substrate xylose. Replacement of aspartate with alanine appears to be a general strategy for improving the activity of *Ct*XR and its homologues towards hydrophobic substrates [24]. By contrast, the W24F and W24Y mutations diminished the reductase activity in the conversion of *rac*-2-phenylpropanal to 6 and 8% of the value of wild-type *Ct*XR, respectively (Table 1). Reduced enzyme activities (with higher K_m-values) towards *rac*-2-phenylpropanal were observed following the removal of the bulky Trp-24, which confirmed a general role of Trp-24 in the efficient conversion of aldehydes. The effects of these single point mutations on the enantioselectivity are discussed below.

Enantioselectivity of *Ct*XR variants towards 2-phenylpropanal

The enantioselectivity of an enzyme is generally defined by the ratio of catalytic efficiencies for the two enantiomers $(E = (k_{cat}/K_{m,S})/(k_{cat}/K_{m,R}))$ [32]. The published racemization velocity (k_{rac}) of 2-phenylpropanal is $75 \cdot 10^{-6}$ s^{-1}, corresponding to a half-life ($t_{1/2}$) of ~ 2 h [15]. The relatively slow racemization should generally enable the determination of the $k_{cat}/K_{m,enantiomer}$ values using enzymatic assays that can be completed in 5 min. However, we observed slow racemization of the pure enantiomers during frozen storage at -18 °C (data not shown). Hence, the enantioselectivities shown in Table 1 (expressed as the $(k_{cat}/K_{m,S})/(k_{cat}/K_{m,rac})$ ratios) represent approximate values that are still useful to guide enzyme selection and reaction optimization. The wild type showed a preference for the (*S*)-aldehyde (ratio of 1.23). The D51A mutant showed a markedly stronger preference for the *S*-enantiomer than the N310A mutant (1.54 vs. 0.77). Asp-51 and Asn-310 are on opposite sides of the substrate-binding pocket (Fig. 3). Asp-51 is suggested to interact with the hydroxyl groups of the natural substrate xylose at C-3, C-4 and C-5, while Asn-310 interacts with the hydroxyl group at C-2 [23] (Fig. 3A). Docking simulations of wild-type *Ct*XR (in complex with NAD$^+$) with (*S*)- and (*R*)-2-phenylpropanal are shown in Fig. 3B. Differential positions of the (*S*)- and (*R*)-2-phenylpropanal enantiomers provide a possible explanation for the

enantiomer preferences of the mutants. Replacement of Asp-51 with alanine might introduce an interaction between the alanine and the phenyl-ring of (*S*)-2-phenylpropanal (Fig. 3C). After replacement of Asn-310 with alanine, this interaction between alanine and the phenyl-ring of (*R*)-2-phenylpropanal becomes even more plausible (Fig. 3D). The W24F and W24Y mutants showed $(k_{cat}/K_{m,S})/(k_{cat}/K_{m,rac})$ ratios of ~ 0.91 (Table 1). along with an approximately ≥ tenfold reduction of their catalytic efficiency. Lower activities (with higher K_m-values) and a preference for the (*R*)-aldehyde might indicate an even poorer interaction between the aromatic rings of phenylalanine or tyrosine and the aldehyde proton of the (*S*)-substrate. In conclusion, the D51A mutant of *Ct*XR was identified as a variant with improved catalytic efficiency and enantioselectivity, exhibiting a ~ 40-fold higher k_{cat} and a ~ 30-fold smaller K_m for the racemic substrate compared to published values for variants of the ADH from *Thermoanaerobacter brockii* [8].

Catalyst stabilization

*Ct*XR is generally known to have low substrate tolerance, with half-lives in the presence of 5 to 10 mM *o*-chloroacetophenone or 1-(2-chlorophenyl)ethanol shorter than 3 min. In the case of *o*-chloroacetophenone and its reaction product, the unfavorable logP values (~ 2) are at least partially responsible for the fast enzyme deactivation. Integration of this oxidoreductase into whole-cell biocatalysts (*E. coli*, *S. cerevisiae*, *C. tenuis*) was previously shown to substantially stabilize the enzyme, resulting in > tenfold improvements of the product titer [34]. Reactive aldehydes are known to form adducts with lysine, histidine and cysteine residues of proteins [29]. Fast enzyme deactivation by 2-phenylpropanal and *o*-chloroacetophenone might therefore be caused by different mechanisms. The use of whole cells provided an extreme case of catalyst stabilization in the presence of 2-phenylpropanal, since the isolated enzyme was deactivated by 0.5 mM aldehyde whereas the whole-cell catalyst was able to tolerate and convert 1 M substrate. Stabilization of the enzyme by whole cells and cell debris was previously reported for the synthesis of (*R*)-phenylacetyl carbinol from benzaldehyde and pyruvate using a pyruvate decarboxylase from *Candida utilis*. The stabilization was ascribed to membrane components that form a microenvironment around the enzyme and thereby decrease aldehyde transfer to the enzyme, protecting it from deactivation at the aqueous/organic interphase [35]. The addition of cyclodextrin (HBC), which was previously shown to boost the reduction of *o*-chloroacetophenone, only had a minor effect on the lyophilized *E. coli* cells used in this study. Catalyst stabilization by cell components was apparently dominant, especially at the higher catalyst

Rapp *et al. BMC Biotechnol*   (2021) 21:58

Page 7 of 13

Table 4 Literature survey of studies on the reductive enzymatic kinetic resolution of rac-2-phenylpropanal

Entry	Bioreduction catalyst, NAD(P)H-recycling strategy	rac-2-phenylpropanal	Reaction medium (auxiliary substrate)	Product (Conversion)	Enantiopurity	Aim of the study	Ref
Horse liver ADH (Zn-containing ADH)							
1	Free enzyme, coupled substrate 1,4-butanediol	5 mM	Buffer pH 7.5, 1% v/v CH$_3$CN, (2.5 mM 1,4-butanediol)	5 mM (98%)	95% ee S	Probing the enzyme's coenzyme recycling ability using the oxidation of 1,4-butanediol into the corresponding lactone	14
2	Free enzyme, coupled substrate ethanol	0.5 mM	Buffer pH 7.5, (0.5 M ethanol)	0.38 mM (75%)	98% ee S	Investigation of DKR, including substrate racemization velocity	10,15
3	Free enzyme, phenylpropanal oxidation for NADH-recycling	75 mM	Buffer pH 7.5; 4% v/v MTBE	28 mM (37%)	96% ee S	Investigation of a biocatalytic asymmetric disproportionation (biocatalytic Cannizzaro reaction)	12
4	Free enzyme, coupled substrate ethanol	165 mM	Buffer, 63% v/v isopropyl ether, (0.6 M ethanol)	82 mM (50%)	96% ee S	Probing the enzyme's enantioselectivity and coenzyme recycling ability	16
5	Free enzyme, coupled substrate ethanol	30 mM	Buffer pH 8, (5% v/v ethanol)	28 mM (93%)	93% ee S	One-pot, two-step reaction: oxidation of rac-2-phenyl-1-propanol into rac-2-phenylpropanal followed by a dynamic enantioselective bioreduction	1
6	Immobilized enzyme, coupled substrate ethanol	5 mM	Buffer pH 7.5, 50% v/v hexane, (0.5 M ethanol)	4.2 mM (84%)	> 98% ee S	Characterization of the immobilized catalyst	17
7	Immobilized enzyme, coupled substrate ethanol	300 mM	Isopropyl ether (saturated with buffer, 0.5% buffer pH 7.0, (1 M ethanol)	46 mM (15%)	95% ee S	Probing the enzyme's substrate scope and enantioselectivity in organic solvents	11
Thermostable ADHs (enzyme superfamily)							
8	Free *Thermoanaerobacter brockii* LG296 ADH mutant (Zn-containing ADH), coupled substrate isopropanol	30 mM	Buffer pH 7.4, (20% v/v isopropanol)	23 mM (75%)	95% ee S	Development of enantioselective mutants	8
9	Free *Thermoanaerobacter brockii* LG277 ADH mutant (Zn-containing ADH), coupled substrate isopropanol	10 mM	Buffer pH 7.4, (20% v/v isopropanol)	7.5 mM (75%)	92% ee R	Development of enantioselective mutants	8
10	Free *Sulfolobus solfataricus* ADH-10 (Zn-containing ADH), coupled substrate ethanol	5 mM	Buffer pH 9, (5% ethanol)	3.7 mM (74%)	98% ee S	Probing the enzyme's substrate scope and enantioselectivity	9
11	Immobilized *Thermus thermophilus* ADH (short-chain dehydrogenases/reductase), coupled enzyme yeast formate dehydrogenase	1 mM	Buffer pH 7, 5% v/v CH$_3$CN (0.1 M formic acid)	1 mM (100%)	71% ee R	Characterization of the immobilized catalyst	13
Other ADHs (enzyme superfamily)							
12	Free *E. coli* ADH (Zn-containing ADH)	30 mM	Buffer pH 8, (5% v/v ethanol)	29 mM (97%)	94% ee S	One-pot, two-step reaction: oxidation of rac-2-phenyl-1-propanol into rac-2-phenylpropanal followed by a dynamic enantioselective bioreduction	1

Rapp *et al. BMC Biotechnol* (2021) 21:58

Page 8 of 13

Table 4 (continued)

Entry	Bioreduction catalyst, NAD(P)H-recycling strategy	rac-2-phenylpropanal	Reaction medium (auxiliary substrate)	Product (Conversion)	Enantiopurity	Aim of the study	Ref
	Origin of enzyme not stated						
13	Free Evo-1.1.200 from Evocatal coupled substrate ethanol	30 mM	Buffer pH 9, (5% v/v isopropanol)	29 mM (95%)	89% ee R	One-pot, two-step reaction: oxidation of rac-2-phenyl-1-propanol into rac-2-phenylpropanal followed by a dynamic enantioselective bioreduction	1
	Whole-cell catalysts						
14	E. coli JM109, NAD(P)H-recycling by native microbial metabolism	22 mM	M9 medium, 30% v/v organic phase (9:1 isopropyl ether: isooctane)	4.4 mM (20%)	~ 50% ee (? unknown)	Probing the host background activity	30
15	CtXR D51A mutant (aldo–keto reductase) coupled enzyme yeast formate dehydrogenase	1000 mM	Buffer pH 7.5, (1.05 M formic acid)	843 mM (98.8%, but product and substrate loss)	93.1% ee S	Process optimization for imroved enantiopurity and yield	This work

Rapp *et al. BMC Biotechnol*   (2021) 21:58

Page 9 of 13

loading of 40 g_{CDW}/L, and the addition of HBC only increased the product concentration at a lower catalyst loading of 20 g_{CDW}/L (Table 3).

Product enantiopurity and concentration

Generally, an enzyme with higher enantioselectivity will generate a product with higher enantiomeric excess. In the case of an enzyme that converts one enantiomer much faster than the other, the product of the initial stage of the conversion at a high substrate and low product concentration will show high enantiopurity, whereas a decrease is expected during the course of the reaction (expressed in the Chen equation, [32]). Hence, product enantiopurity depends on the enantioselectivity of the reductase and on the availability (concentrations) of both substrate enantiomers. DKR strategies make use of the relatively fast racemization of 2-aryl-1-propanals (reviewed in Kourist et al. [4]). Optimally, there is an equal availability of both substrate enantiomers during the entire DKR reaction (both substrate enantiomers are present in equal concentrations). However, in the present case, a relatively high reductase activity was used to compensate for fast catalyst deactivation, leading to a trade-off between the enantiomeric purity and final titer of the product (Fig. 2). A dependence of product enantiopurity on reaction progress, especially at high enzyme loading, was also reported in other studies on DKR. The substrate racemization velocity was previously identified as the main factor limiting product enantiopurity [12]. Here, the substrate-to-catalyst ratio was identified as the main factor determining product enantiopurity. The *ee* value of the product showed the expected dependence on the substrate-to-catalyst ratio (expressed as $g_{substrate}$/g_{CDW} in Fig. 4). The highest *ee*-values of 95.3 and 95.4 were obtained for the conversions of 100 and 2 M *rac*-2-phenylpropanal by 4 and 40 g_{CDW}/L, respectively. However, the reduction of 2 M substrate was compromised by a low conversion ratio (~ 30%, Table 3). Thus, a compromise between product enantiopurity and the conversion ratio had to be found. Overall, the main limiting factors were substrate racemization velocity, catalyst stability and catalyst loading, with higher catalyst loading leading to a loss of the hydrophobic product in the biomass fraction during downstream processing [36].

Conclusions

Detailed optimization of a reductive enzymatic dynamic kinetic resolution of racemic 2-phenylpropanal yielded 843 mM (115 g/L) (*S*)-2-phenylpropanol with 93% *ee*. The multilevel strategy included rational mutagenesis of *Ct*XR for improved enzyme activity and enantioselectivity, the use of an *E. coli* whole-cell catalyst for enzyme stabilization and coenzyme recycling, as well as the

optimization of the substrate-to-catalyst ratio to increase the enantiopurity and final titer of the product. The use of the whole-cell catalyst led to a remarkable > 1000-fold improvement of the product concentration, indicating strong enzyme stabilization by cellular components. The most important factor for obtaining high enantiopurities and product concentrations was the ratio of substrate to catalyst (Fig. 4). High reduction velocities led to high conversions at the expense of lower product enantiopurities. The conversion with a catalyst loading of 40 g_{CDW}, 10 mM NAD^+ and 1 M substrate was identified as a suitable compromise, affording 843 mM (*S*)-phenylpropanol with 93.1% *ee* (Table 3).
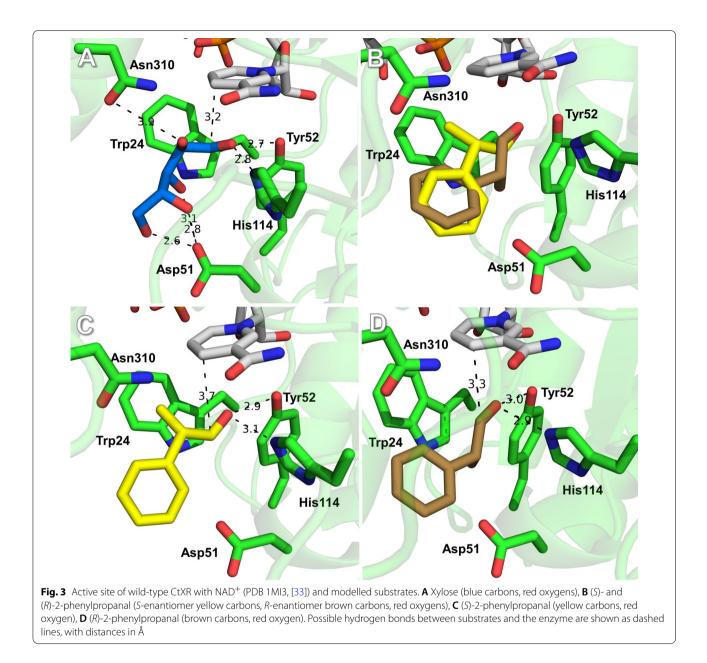
Materials and methods
Chemicals, enzymes and strains

Racemic 2-phenylpropanal (98%), racemic 2-phenylpropanol (97%), acetophenone (99%) and racemic 1-phenylethanol ($\geq$ 98%) were purchased from Sigma-Aldrich/Fluka (Vienna, Austria); (*S*)-2-phenylpropanal (95%) and (*R*)-2-phenylpropanal (95%) were from Accela (Prien – Chiemsee, Germany); 2-hydroxypropyl-β-cyclodextrin (HBC, batch number OH053931501) was from Carbosynth (Berkshire, UK); NAD^+ (98%), acetonitrile ($\geq$ 99) and ethyl acetate ($\geq$ 99,9%) were from Roth (Karlsruhe, Germany). Other chemicals were from Sigma-Aldrich/Fluka or Roth, and were of the highest purity available. Materials for genetic modification were reported elsewhere [24]. The used reductases were the wild type and single-point mutants of *Candida tenuis* xylose reductase (*Ct*XR wild-type GenBank ID AF074484). Site-directed mutagenesis for the construction of the *Ct*XR mutants D51A, W24F, W24Y, N310A, and N310D was carried out using inverse PCR as described elsewhere [24]. The protein expression of *Ct*XR (wild-type and mutants D51A, W24F, W24Y, N310A, N310D) was described previously [24]. An *E. coli* Rosetta2 strain co-expressing *Ct*XR D51A and *Cb*FDH (GenBank ID AJ011046) was used in the bioreductions. The construction of the co-expression strain was previously described by Rapp et al. [19]. Cultivation of the co-expression strain was described previously [19], and is summarized in the Additional file 1. The biomass was frozen at −20 °C, lyophilized (Christ α 1–4 lyophilizer from Braun Biotech International) and stored at −20 °C.

Enzyme kinetics

Steady state kinetic parameters for the NADH-dependent reduction of 2-phenylpropanal by *Ct*XR variants were determined spectrophotometrically as described earlier [24]. The solubility of 2-phenylpropanal in water was increased to 0.5 mM by the addition of 25% v/v DMSO.
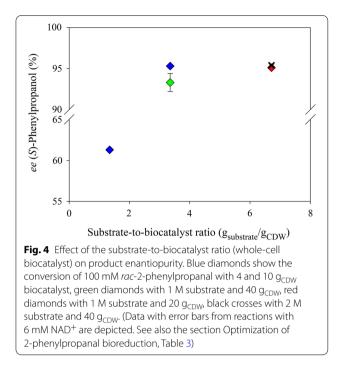
Rapp *et al. BMC Biotechnol*   *(2021) 21:58*

Page 10 of 13

Fig. 3 Active site of wild-type CtXR with NAD$^+$ (PDB 1MI3, [33]) and modelled substrates. **A** Xylose (blue carbons, red oxygens), **B** (*S*)- and (*R*)-2-phenylpropanal (*S*-enantiomer yellow carbons, *R*-enantiomer brown carbons, red oxygens), **C** (*S*)-2-phenylpropanal (yellow carbons, red oxygen), **D** (*R*)-2-phenylpropanal (brown carbons, red oxygen). Possible hydrogen bonds between substrates and the enzyme are shown as dashed lines, with distances in Å

Substrate solutions were freshly prepared and immediately used to avoid non-enzymatic decomposition or racemization in aqueous solution in the case of (*S*)-2-phenylpropanal. A typical measurement period was 5 min. Non-specific background activity was taken into account by measuring blank mixtures. The added DMSO had no effect on the enzyme's activity with the natural substrate D-xylose.

Bioreduction of racemic 2-phenylpropanal
Reduction by the isolated CtXR D51A
Racemic 2-phenylpropanal was dissolved in DMSO prior to dilution into 50 mM potassium phosphate buffer, pH

7.0, to a final DMSO concentration of 25%. The substrate (final concentration 0.5 mM) was incubated at 25 °C in the presence of 0.2 mM NADH and *Ct*XR D51A for 2 h. For time-course analysis, 100-μL samples were taken from the reaction mixtures (final reaction volume 1.5 mL) at the specified timepoints. All samples were diluted 1:1 with acetonitrile and centrifuged prior to analysis by chiral HPLC.

Whole-cell bioreductions
Lyophilized biomass (40 mg or 80 mg) was rehydrated in 1 mL of potassium phosphate buffer (100 mM, pH 6.2)

Fig. 4 Effect of the substrate-to-biocatalyst ratio (whole-cell biocatalyst) on product enantiopurity. Blue diamonds show the conversion of 100 mM *rac*-2-phenylpropanal with 4 and 10 g_{CDW} biocatalyst, green diamonds with 1 M substrate and 40 g_{CDW}, red diamonds with 1 M substrate and 20 g_{CDW}, black crosses with 2 M substrate and 40 g_{CDW}. (Data with error bars from reactions with 6 mM NAD^+ are depicted. See also the section Optimization of 2-phenylpropanal bioreduction, Table 3)

containing NAD^+ (0.5−14 mM) and sodium formate (50 mM, excess over substrate) in 2 mL Eppendorf tubes. Activities of the whole biomass, measured after cell lysis and protein extraction for *rac*-2-phenylpropanal reduction and formate dehydrogenase were 2200 and 154 U/g_{CDW}, respectively [19]. *rac*-2-phenylpropanal reduction activity was determined at 0.5 mM *rac*-2-phenylpropanal in 50 mM potassium phosphate buffer, pH 7.0, with 25% DMSO. The rehydrated biomass (containing NAD^+ and sodium formate, volume of the biomass slurry ≤ 50% v/v of the total bioreduction mixture) was combined with the substrate and filled up to a total working volume of 1 mL. In case of cyclodextrin-aided conversions, HBC and substrate were weighed separately in Eppendorf tubes containing 50 μL buffer, followed by vortexing prior to addition to the biomass. Eppendorf tubes were sealed with parafilm and vortexed until the mixtures completely emulsified. The mixtures were reacted for 24 or 48 h at room temperature using an end-over-end rotator (30 rpm). The fed-batch bioreductions were started as batch reactions with 330 mM substrate, 6 mM NAD^+ and 40 g_{CDW}/L. 50 μL *rac*-2-phenylpropanal, and were fed after 2 and 4 h to reach a total substrate concentration corresponding to 1 M. The reaction was carried out for 48 h.

Substrate/product recovery
For recovery experiments at substrate/product concentrations of 1 M, reaction mixtures containing 20 or 40 g_{CDW}/L catalyst were prepared without adding NAD^+.

The samples were incubated under the same conditions as used for biotransformations and extracted following the procedure described in Sect. Analytical methods. Substrate/product recovery was performed in duplicates.

Analytical methods
For HPLC and GC analyses, ethyl acetate (1 mL) was added to 1 mL of a reaction mixture in a 2 mL Eppendorf tube. The tubes were vortexed and the mixtures transferred into 15 mL Sarstedt tubes. The tubes were then filled up to 10 mL with ethyl acetate, vortexed and centrifuged for 15 min, 25 °C and 3220 g for extraction. Final dilutions in ethyl acetate contained 5 mM substrate/product. For NMR analyses, substrate/product present in ethyl acetate after extraction was transferred into round-flasks and evaporated under reduced pressure. The isolated substrate/product was directly dissolved in deuterated methanol (20 μL substrate/product + 680 μL solvent).

Chiral HPLC analysis
HPLC analysis was performed using a Merck-Hitachi LaChrom HPLC system equipped with a Merck L-7490 RI detector, an L-7400 UV-detector, a reversed phase Chiralpak® AD-RH column (from Daicel, obtained at Sigma Aldrich, Vienna, Austria) and a thermostat column oven (40 °C). The mobile phase was composed of 25% acetonitrile in ddH_2O at a flowrate of 30 mL/min. HPLC standard curves were prepared using racemic product at 0.1, 0.5, 1, 5, and 10 mM concentrations. Peak areas at corresponding retention times were used to calculate the concentrations. The enantiomeric excess of the major product (*S*)-2-phenylpropanol was calculated using the formula $ee = (S\text{-alcohol} − R\text{-alcohol})/(S\text{-alcohol} + R\text{-alcohol})$. The retention times and chromatograms of authentic standards (main products ((*S*)-2-phenylpropanol, (*R*)-2-phenylpropanol), by-products (acetophenone, phenylethanol) were summarized in the Additional file 1: Sect. 4. The aldehydes gave too broad peaks on HPLC and were quantified by GC-FID.

Chiral GC-FID analysis
GC analysis was performed on an Agilent 7890A GC with FID detection [12] equipped with a chiral Hydrodex®-β-TBDAc column with 25 m length and an inner diameter of 0.25 mm (from Macherey–Nagel obtained from FisherScientific, Austria, Vienna). The carrier gas was H_2 with a flow of 1 mL/mi, the injection volume was 5 μL, the split ratio was 50:1, the inlet temperature 230 °C, and the detector temperature 250 °C. The following temperature program was used for the separation of analytes: 110 °C/hold 10 min; 2 °C per min to 123 °C/hold 3 min; 10 °C per min to 200 °C/hold 1 min. The retention times and

Rapp *et al. BMC Biotechnol*   (2021) 21:58

Page 12 of 13

chromatograms of authentic standards (main products ((*S*)-2-phenylpropanol, (*R*)-2-phenylpropanol), substrate ((*S*)-2-phenylpropanal, (*R*)-2-phenylpropanal) by-products (acetophenone, phenylethanol) are summarized in the Additional file 1: Sect. 5.

NMR analysis
^{1}H-NMR spectra of isolated substrate/product from biotransformations (78% conversion) were recorded using a 300 MHz Bruker NMR unit (300 MHz for ^{1}H) at 300 K. Chemical shifts (δ) were depicted in ppm relative to the resonance of the solvent (MeOD) (see also Additional file 1: Sect. 6).

Enzyme–substrate docking simulations
PyMOL Molecular Graphics System (Open-Source, Schrödinger, LLC) was used for enzyme/ligand structure depictions. Ligand docking simulations were performed in YASARA (YASARA Biosciences GmbH, Vienna, Austria) using AutoDock Vina [37] with standard parameters.

Abbreviations
ADH: Alcohol dehydrogenase; *Cb*FDH: *Candida boidinii* Formate dehydrogenase; *Ct*XR: *Candida tenuis* Xylose reductase; DKR: Dynamic kinetic resolution; g$_{CDW}$: Cell dry weight in gram; HBC: 2-Hydroxypropyl-β-cyclodextrin; HLADH: Horse liver alcohol dehydrogenase; *rac*: Racemic.

Supplementary Information
The online version contains supplementary material available at https://doi.org/10.1186/s12896-021-00715-5.

Additional file 1. 1. Biomass production. 2. Reduction of *rac*-2-phenylpropanal by isolated *Ct*XR D51A. Time course of the reduction of 0.5 mM substrate with 240 U/mL of isolated *Ct*XR D51A. 3. Biotransformation of *rac*-2-phenylpropanal. Conversions and product *ee*-values from the reduction of 100 mM *rac*-2-phenylpropanal using a lyophilized and rehydrated whole-cell catalyst. Effects of catalyst loading. Conversions and product *ee*-values from the reduction of 1 M *rac*-2-phenyl-propionaldehyde using a lyophilized and rehydrated whole-cell catalyst. Effects of catalyst loading (20 g$_{CDW}$/L, 40 g$_{CDW}$/L) and coenzyme concentration (NAD$^+$ 3–14 mM). (The data are based on HPLC measurements, Table 3). 4. Reversed phase chiral HPLC. Separation of main products and by-products by HPLC. UV traces and retention times for *rac*-2-phenylpropanal, acetophenone, 1-phenylethanol, (*R,S*)-2-phenylpropanol, reaction buffer with NAD$^+$, reaction buffer, bioreduction sample of 1 M *rac*-2-phenylpropanal reacted with 40 g$_{CDW}$/L and 6 mM NAD$^+$. 5. Chiral GC-FID. GC traces and retention times for main products, by-products and bioreduction replicates (N = 6) of 1 M *rac*-2-phenylpropanal reacted with 40 g$_{CDW}$/L and 6 mM NAD$^+$. 6. ^{1}H-NMR. ^{1}H-spectrum of the isolated product from a reaction with 78% analytical yield (HPLC) from 1 M *rac*-2-phenylpropanal reacted with 40 g$_{CDW}$/L and 6 mM NAD$^+$.

Declarations

Ethics approval and consent to participate
Not applicable.

Consent for publication
Not applicable.

Competing interests
The authors declare that they have no competing interests.

Author details
^{1}Institute of Biotechnology and Biochemical Engineering, Graz University of Technology, NAWI Graz, 8010 Graz, Austria. ^{2}Department of Chemistry, University of Graz, NAWI Graz, Heinrichstrasse 28, 8010 Graz, Austria. ^{3}Austrian Centre of Industrial Biotechnology (ACIB), 8010 Graz, Austria.

References
1. Díaz-Rodríguez A, Ríos-Lombardía N, Sattler JH, Lavandera I, Gotor-Fernández V, Kroutil W, Gotor V. Deracemisation of profenol core by combining laccase/TEMPO-mediated oxidation and alcohol dehydrogenase-catalysed dynamic kinetic resolution. Catal Sci Technol. 2015;5:1443–6. https://doi.org/10.1039/C4CY01351D.
2. Abate A, Brenna E, Fuganti C, Gatti FG, Giovenzana T, Malpezzi L, Serra S. Chirality and fragrance chemistry: stereoisomers of the commercial chiral odorants Muguesia and Pamplefleur. J Org Chem. 2005;70:1281–90. https://doi.org/10.1021/jo048445j.
3. Scognamiglio J, Jones L, Letizia CS, Api AM. Fragrance material review on β-methylphenethyl alcohol. Food Chem Toxicol. 2012;50:199–203. https://doi.org/10.1016/j.fct.2011.10.023.
4. Kourist R, Domínguez de María P, Miyamoto K. Biocatalytic strategies for the asymmetric synthesis of profens—recent trends and developments. Green Chem. 2011;13:2607–2618; https://doi.org/10.1039/C1GC15162B.
5. Carvalho PO, Cass QB, Calafatti SA, Contesini FJ, Bizaco R. Review- Alternatives for the separation of drug enantiomers: ibuprofen as a model compound. Braz J Chem Eng. 2006;23:291–300. https://doi.org/10.1590/S0104-66322006000300003.
6. Koul S, Parshad R, Taneja SC, Qazi GN. Enzymatic resolution of naproxen. Tetrahedron Asymmetry. 2003;14:2459–65. https://doi.org/10.1016/S0957-4166(03)00492-0.
7. Steenkamp L, Brady D. Optimisation of stabilised carboxylesterase NP for enantioselective hydrolysis of naproxen methyl ester. Process Biochem. 2008;43:1419–26. https://doi.org/10.1016/j.procbio.2008.09.001.

Rapp *et al. BMC Biotechnol*   (2021) 21:58

Page 13 of 13

8. Dong Y, Yao P, Cui Y, Wu Q, Zhu D, Li G, Reetz MT. Manipulating the stereoselectivity of a thermostable alcohol dehydrogenase by directed evolution for efficient asymmetric synthesis of arylpropanols. Biol Chem. 2019;400:313–21. https://doi.org/10.1515/hsz-2018-0299.

9. Friest JA, Maezato Y, Broussy S, Blum P, Berkowitz DB. Use of a robust dehydrogenase from an archael hyperthermophile in asymmetric cataly-sis—dynamic reductive kinetic resolution entry into (*S*)-Profens. J Am Chem Soc. 2010;132:5930–1. https://doi.org/10.1021/ja910778p.

10. Giacomini D, Galletti P, Quintavalla A, Gucciardo G, Paradisi F. Highly efficient asymmetric reduction of arylpropionic aldehydes by Horse Liver Alcohol Dehydrogenase through dynamic kinetic resolution. Chem Com-mun. 2007;4038–4040; doi:https://doi.org/10.1039/B712290J.

11. Grunwald J, Wirz B, Scollar MP, Klibanov AM. Asymmetric oxidoreductions catalyzed by alcohol dehydrogenase in organic solvents. J Am Chem Soc. 1986;108:6732–4. https://doi.org/10.1016/s0958-1669(03)00074-0.

12. Tassano E, Faber K, Hall M. Biocatalytic parallel interconnected dynamic asymmetric disproportionation of α-substituted aldehydes: atom-efficient access to enantiopure (*S*)-Profens and Profenols. Adv Synth Catal. 2018;360:2742–51. https://doi.org/10.1002/adsc.201800541.

13. Rocha-Martín J, Vega D, Bolivar JM, Hidalgo A, Berenguer J, Guisán JM, López-Gallego F. Characterization and further stabilization of a new anti-prelog specific alcohol dehydrogenase from *Thermus thermophilus* HB27 for asymmetric reduction of carbonyl compounds. Bioresour Technol. 2012;103:343–50. https://doi.org/10.1016/j.biortech.2011.10.018.

14. Kara S, Spickermann D, Schrittwieser JH, Leggewie C, van Berkel WJH, Arends IWCE, Hollmann F. More efficient redox biocatalysis by utilizing 1,4-butanediol as a "smart cosubstrate." Green Chem. 2013;15:330–5. https://doi.org/10.1039/C2GC36797A.

15. Galletti P, Emer E, Gucciardo G, Quintavalla A, Pori M, Giacomini D. Chem-oenzymatic synthesis of (2*S*)-2-arylpropanols through a dynamic kinetic resolution of 2-arylpropanals with alcohol dehydrogenases. Org Biomol Chem. 2010;8:4117–23. https://doi.org/10.1039/C005098A.

16. Kelemen-Horváth I, Nemestóthy N, Bélafi-Bakó K, Gubicza L. Stereoselec-tive reduction of 2-phenylpropionaldehyde by alcohol dehydrogenase with cofactor regeneration. Chem Papers. 2002;56:52–6.

17. Quaglia D, Pori M, Galletti P, Emer E, Paradisi F, Giacomini D. His-tagged horse liver alcohol dehydrogenase: Immobilization and application in the bio-based enantioselective synthesis of (*S*)-arylpropanols. Process Biochem. 2013;48:810–8. https://doi.org/10.1016/j.procbio.2013.03.016.

18. Kratzer R, Nidetzky B. Identification of *Candida tenuis* xylose reductase as highly selective biocatalyst for the synthesis of aromatic α-hydroxyesters and improvement of its efficiency by protein engineering. Chem Com-mun. 2007;10:1047–9. https://doi.org/10.1039/B616475G.

19. Rapp C, Nidetzky B, Kratzer R. Pushing the limits: Cyclodextrin-based intensification of bioreductions. J Biotechnol. 2021;325:57–64. https://doi.org/10.1016/j.jbiotec.2020.11.017.

20. Couture J-F, Legrand P, Cantin L, Labrie F, Luu-The V, Breton R. Loop relaxa-tion, a mechanism that explains the reduced specificity of rabbit 20alpha-hydroxysteroid dehydrogenase, a member of the aldo-keto reductase superfamily. J Mol Biol. 2004;339:89–102. https://doi.org/10.1016/j.jmb.2004.03.035.

21. Krump C, Vogl M, Brecker L, Nidetzky B, Kratzer R. Acceleration of an aldo-keto reductase by minimal loop engineering. PEDS. 2014;27:245–8. https://doi.org/10.1093/protein/gzu021.

22. Qiu S, Cheng F, Jin L-J, Chen Y, Li S-F, Wang Y-J, Zheng Y-G. Co-evolution of activity and thermostability of an aldo-keto reductase *Km*AKR for asym-metric synthesis of statin precursor dichiral diols. Bioorg Chem. 2020;103: 104228. https://doi.org/10.1016/j.bioorg.2020.104228.

23. Kavanagh KL, Klimacek M, Nidetzky B, Wilson DK. The structure of apo and holo forms of xylose reductase, a dimeric aldo-keto reductase from *Candida tenuis*. Biochemistry. 2002;41:8785–95. https://doi.org/10.1080/15216540600818143.

24. Kratzer R, Leitgeb S, Wilson DK, Nidetzky B. Probing the substrate bind-ing site of *Candida tenuis* xylose reductase (AKR2B5) with site-directed mutagenesis. Biochem J. 2006;393:51–8. https://doi.org/10.1042/BJ20050831.

25. Leis D, Lauß B, Macher-Ambrosch R, Pfennig A, Nidetzky B, Kratzer R. Integration of bioreduction and product isolation: Highly hydrophobic co-solvents promote *in situ* substrate supply and extractive product isola-tion. J Biotechnol. 2017;257:110–7. https://doi.org/10.1016/j.jbiotec.2016.11.021.

26. Fuchs CS, Hollauf M, Meissner M, Simon RC, Besset T, Reek JNH, Riethorst W, Zepeck F, Kroutil W. Dynamic kinetic resolution of 2-phenylpropanal derivatives to yield β-chiral primary amines via bioamination. Adv Synth Catal. 2014;356:2257–65. https://doi.org/10.1002/adsc.201400217.

27. Vogl M, Kratzer R, Nidetzky B, Brecker L. *Candida tenuis* xylose reductase catalysed reduction of acetophenones: the effect of ring-substituents on catalytic efficiency. Org Biomol Chem. 2011;9:5863–70. https://doi.org/10.1039/C1OB05510K.

28. Könst P, Merkens H, Kara S, Kochius S, Vogel A, Zuhse R, Holtmann D, Arends IWCE, Hollmann F. Enantioselective oxidation of aldehydes cata-lyzed by alcohol dehydrogenase. Angew Chemie Int Ed. 2012;51:9914–7. https://doi.org/10.1002/anie.201203219.

29. LoPachin RM, Gavin T. Molecular mechanisms of aldehyde toxicity: a chemical perspective. Chem Res Toxicol. 2014;27:1081–91. https://doi.org/10.1021/tx5001046.

30. Sello G, Orsini F, Bernasconi S, Di Gennaro P. Selective enzymatic reduc-tion of aldehydes. Molecules. 2006;11:365–9. https://doi.org/10.3390/11050365.

31. Karlsson A, El-Ahmad M, Johansson K, Shafqat J, Jörnvall H, Eklund H, Ramaswamy S. Tetrameric NAD-dependent alcohol dehydrogenase Chem-Biol Interact. 2003;143–144:239–45.

32. Chen S, Fujimoto Y, Girdaukas G, Sih CJ. Quantitative analyses of biochem-ical kinetic resolutions of enantiomers. J Am Chem Soc. 1982;104:7294–9. https://doi.org/10.1021/ja00389a064.

33. Kavanagh KL, Klimacek M, Nidetzky B, Wilson DK. Structure of xylose reductase bound to NAD+ and the basis for single and dual co-substrate specificity in family 2 aldo-keto reductases. Biochem J. 2003;373:319–26. https://doi.org/10.1042/bj20030286.

34. Kratzer R, Woodley JM, Nidetzky B. Rules for biocatalyst and reaction engineering to implement effective, NAD(P)H-dependent, whole cell bioreductions. Biotechnol Adv. 2015;33:1641–52. https://doi.org/10.1016/j.biotechadv.2015.08.006.

35. Satianegara G, Rogers PL, Rosche P. Comparative studies on enzyme preparations and role of cell components for (*R*)-phenylacetylcarbinol production in a two-phase biotransformation. Biotechnol Bioeng. 2006;94:1189–95. https://doi.org/10.1002/bit.20959.

36. Lauß B, Rapp C, Leis D, Nidetzky B, Kratzer R. Separation behavior and microstructure of emulsified, two-phasic *E. coli* bioreaction mixtures. Colloids Interface Sci Commun. 2020;35:100248; doi:https://doi.org/10.1016/j.colcom.2020.100248.

37. Trott O, Olson AJ. AutoDock Vina: Improving the speed and accuracy of docking with a new scoring function, efficient optimization and multi-threading. J Comput Chem. 2009;31:455–61. https://doi.org/10.1002/jcc.213.

Publisher's Note